

Fabrication of graphite-graphene-ionic liquid modified carbon nanotubes filled natural rubber thin films for microwave and energy storage applications

Srinivasarao Yaragalla¹ · Bashaiah Sindam² · Jiji Abraham¹ · K. C. James Raju² · Nandakumar Kalarikkal^{1,3} · Sabu Thomas^{1,4}

Received: 22 November 2014 / Accepted: 1 June 2015 / Published online: 21 June 2015
© Springer Science+Business Media Dordrecht 2015

Abstract Exploiting polymer nanocomposites as dielectric and heat storage devices is an important approach to develop high performance materials. Graphite (GT), thermally reduced graphene oxide (TRG), and hybrid consisting of TRG and ionic liquid (1-Ethyl-2, 3-dimethylimidazolium bis (trifluoromethylsulfonyl) imide) modified carbon nanotubes (IMCNT) were added to natural rubber and membranes were fabricated via melt mixing method. The amount of the GT, TRG, TRG+IMCNT used in this work was in the range of 0.5 to 5 wt%. Mechanical properties of NR nanocomposites revealed that the hybrid (TRG+IMCNT) (5 wt%) system showed high tensile strength, high modulus and low elongation at break as compared to neat NR, NR reinforced with GT (5 wt%) and NR reinforced with TRG (5 wt%) systems owing to the synergistic hybrid effect caused by the network formation of the hybrid fillers inside NR matrix. Dielectric properties of

the prepared membranes were studied at 2.5, 10 and 20 GHz in the microwave frequency region using a Split Post Dielectric Resonator (SPDR) based technique. The incorporation of micro and nanofillers in the natural rubber (NR) matrix results in consistent improvement in dielectric constant and lower loss tangent values. In certain cases the samples containing 5 wt% of filler exhibited high loss or conducting behaviour at higher frequencies (10 and 20 GHz). Different techniques had to be employed for measuring the dielectric constant and loss tangent of the prepared membranes where they showed a high loss or conducting behaviour. Moreover, thermal history like glass transition temperature and the change in heat capacity were estimated using Differential Scanning Calorimetry (DSC). In addition, the dispersion of micro and nanofillers inside the NR was estimated using X-ray followed by Transmission Electron Microscopy for the morphology architecture of nanofillers. The morphology of the prepared membranes was correlated with the mechanical, dielectric and thermal properties. The hybrid system (TRG+IMCNT) exhibited high dielectric constant (5.6) and low heat capacity value (0.32 J/g°C) as compared to GT and TRG systems.

-
- ✉ K. C. James Raju
kcjrsp@uohyd.ernet.in
- ✉ Nandakumar Kalarikkal
nkkalarikkal@mgu.ac.in
- ✉ Sabu Thomas
sabupolymer@yahoo.com

Keywords Thermally reduced graphene oxide · Carbon nanotube · Graphite · Natural rubber

- ¹ International and Inter University Centre for Nanoscience and Nanotechnology, Mahatma Gandhi University, Kottayam 686560, Kerala, India
- ² School of Physics, University of Hyderabad, Hyderabad 500046, Telengana, India
- ³ School of Pure and Applied Physics, Mahatma Gandhi University, Kottayam 686560, Kerala, India
- ⁴ School of Chemical Sciences, Mahatma Gandhi University, Kottayam 686560, Kerala, India

Introduction

Nano fillers which are especially generated from carbon such as carbon black, fullerenes, graphenes, carbon nanotubes, and graphite platelets have been attracting much attention in polymer composites owing to their excellent electrical, mechanical and optical properties [1–9]. The incorporation of these micro and nanofillers into the polymers led to the formation of heterogeneous hybrid materials having both nanofiller and

polymer properties. These kind of materials can be useful for manifold applications in electrical engineering, automobiles etc. The main purpose here is to add these nanofillers into polymers to reduce the cost of the material and to achieve better properties compared to bulk polymers. At present, graphenes and carbon nanotubes are gaining a lot of interest among the carbon based fillers because of their abnormal electrical and mechanical properties which had lead to the fabrication of flexible energy storage devices, conductors for sensing applications [10–13]. Graphene is a two dimensional sheet filler and all carbon atoms are arranged in the hexagonal geometry. An unabated issue regarding graphene is its electrical property which is induced by the delocalization of π electrons at room temperature. Carbon nanotubes are generated from graphenes via wrapping of carbon nanotubes. The structural arrangements of carbon atoms are same as that in graphene. The main discrepancy between graphene and carbon nanotube (CNT) is that graphene is a sheet shaped and CNT is a rod shaped material. The end of the CNT tube carbon can exist in sp^2 and sp^3 hybridizations.

The materials which can absorb or store microwave energy are much beneficial for various applications like microwave signal detectors (antenna, radars) and energy storage, sensing devices. Many research reports have been published on graphene and CNT filled polymer composites [14–17]. Core amount of research work has been devoted to microwave dielectric properties of CNT filled polymer composites [18–20]. However, to date, no study has been unveiled based on graphene and ionic liquid modified multi walled carbon nanotubes (IMCNTs) hybrid filled natural rubber (NR) system associated with dielectric studies at microwave frequencies. First Omar et al. [21] have reported microwave studies based on carbon black and graphene filled natural rubber composites and they limited the frequency region up to 12 GHz. They used graphene from Hayzen Engineering Co. Ankara, and the maximum amount incorporated was 10 wt%. They have achieved a maximum dielectric constant of 2.5 at the lower frequency range [21, 22].

In our present study, we have modified the multiwalled carbon nanotubes using ionic liquid (1-Ethyl-2, 3-dimethylimidazolium bis (trifluoromethylsulfonyl) imide) and synthesized thermally reduced graphene oxide (TRG) by Hummer method. Thereafter, graphite (GT), TRG and hybrid TRG+IMCNTs filled natural rubber, thin films have been fabricated by melt mixing method. The dielectric properties (at microwave frequencies) and their thermal properties (especially change in heat capacity) were compared and correlated with their developed morphologies. Besides, the state of dispersion of these nanofillers inside NR was evaluated using Wide angle X-ray scattering (WAXS) and connected with the achieved mechanical, microwave and thermal (heat capacity) properties.

Materials and experimental methods

Materials

Natural rubber (ISNR-5) was received from Rubber Research Institute of India, Kottayam, Kerala. The number average molecular weight of natural rubber is around 1×10^6 . Graphite powder, $KMnO_4$, $NaNO_3$, H_2SO_4 , and 30 % H_2O_2 were received from Merck. Multi walled carbon nanotubes and 1-Ethyl-2,3-dimethylimidazolium bis(trifluoromethylsulfonyl) imide ionic liquid were received from Nanocyl, Belgium.

Modification of multi walled carbon nanotubes using 1-Ethyl-2, 3-dimethylimidazolium bis (trifluoromethylsulfonyl) imide ionic liquid

Multi walled carbon nanotubes were mixed with ionic liquid in the ratio of 1:3. It implies that 1 g CNT mixed with 3 mmol of ionic liquid (1 mmol=Molecular weight/1000). CNT and ionic liquid were ground physically in an agate mortar for 30 min and then sonicated using bath sonicator for 30 min in ethanol. Thereafter, evaporated the solvent at room temperature and finally dried in vacuum oven at 50 °C.

Preparation of thermally reduced graphene oxide

Initially graphene oxide was prepared by Hummer method [23] and is well-documented in literature. Thereafter, graphene oxide was taken into a crucible and kept the inside furnace for thermal exfoliation at 200 °C for 1 h.

Preparation of NR polymer nanocomposites

To fabricate NR-GT, NR-TRG, and NR-(TRG+IMCNT) composites, initially Haake melt mixer was used to mix NR and the filler TRG at 125 °C for 10 min. Afterwards, the curatives were added to the NR-TRG mixture within the melt mixer and the mixing was continued around 15 min. The mixed formulation of composites is shown in Table 1. The TRG was added at five different loading of 0.5, 1, 2, 3 and 5 wt%. In a similar way NR-GT and NR-(TRG+IMCNTs) composites were fabricated.

Characterization

Raman spectroscopy

TRG and IMCNT were characterized using Horiba JobinYvon, HR800 PL-Raman spectroscopy and the wavelength of the laser used was 513 nm.

Table 1 Formulations of NR composites (amounts are taken in % W/W ratio)

TRG	NR	ZnO	Stearic acid	TMTM	TQ	CBS	Sulphur
0	100	5	2	0.1	3	1.5	2.5
0.5	100	5	2	0.1	3	1.5	2.5
1	100	5	2	0.1	3	1.5	2.5
2	100	5	2	0.1	3	1.5	2.5
3	100	5	2	0.1	3	1.5	2.5
4	100	5	2	0.1	3	1.5	2.5

Wide angle X-ray scattering (WAXS)

The TRG and NR-TRG composites were characterized by XRD (D8-Advance of Bruker, Germany). The energy of the radiation was 8.04 keV and wavelength 1.54 Å.

Transmission electron microscopy (TEM)

The morphology was analyzed by TEM (JEOL), TRG powder (0.5 mg) was sonicated using a bath sonicator for 5 min in THF solvent and then drop cast on TEM grid. The polymer composite samples were cryogenically cut prior to analysis using an ultramicrotome (Leica, Ultracut UCT).

Mechanical testing

The mechanical properties of the selected NR composites were performed using Universal Testing Machine (Tinius Olsen H50KT).

Differential Scanning Calorimetry (DSC)

TA instrument DSC Q200 was used to investigate the thermal properties of NR-TRG composites. It was calibrated with Indium as standard prior to analysis under nitrogen atmosphere. Each sample was equilibrated at -100 °C then heated to 30 °C and completed the three cycles.

Microwave dielectric properties

The microwave dielectric properties of these NR polymer composites were determined using an Agilent 8722 ES vector network analyzer by employing the Split Post Dielectric Resonator (SPDR) based measurement technique [24]. The SPDR based measurement technique gives a high accuracy for measurement of complex permittivity of thin sheets of insulators at spot frequencies in the frequency range of 1–20 GHz. The SPDR operates with the TE₀₁ mode, which has only the azimuthal electric field component so the electric field remains continuous on the dielectric interfaces. The measurement is carried out for unloaded quality factor and resonance

frequency of a resonator with and without sample. The unloaded Q-factor depends on the conductor and dielectric losses and related parameters. The complex permittivity can be derived using measured resonant frequencies, quality factor and physical dimensions. For this purpose one has to measure the resonance frequency and quality factor (f₀, Q₀₁) of the empty resonator and do the same (f_s, Q_s) with the thin sample. The real part of permittivity of the sample is found on the basis of the measurements of the resonant frequencies and the thickness of the sample as an iterative solution to Eq. (1).

$$\epsilon = \frac{1 + (f_0 + f_s)}{hf_0K_s(\epsilon, h)} \tag{1}$$

Here, h is the sample thickness, f₀ is the resonance frequency of the SPDR without the thin sample, and f_s is the resonance frequency of the SPDR with the sample. K_s is a function of the sample’s dielectric constant ε_r and thickness h. Since K is a slowly varying function of ε_r and h, the iterations using the formula (1) converge rapidly. The loss tangent is computed using the Eq. (2):

$$\tan\delta = \frac{Q^{-1} - Q_{Dr}^{-1} - Q_c^{-1}}{P_{es}} \tag{2}$$

where, Q is the unloaded Q factor of the SPDR containing the dielectric sample and P_{es} is the electrical energy-filling factor of the sample. Q_c is the Q factor corresponding to metal losses of the SPDR containing the dielectric sample and Q_{Dr} is the Q-factor corresponding to the dielectric losses in the dielectric resonators of SPDR set-up.

Results and discussion

Characterization of ionic liquid modified multi walled carbon nanotubes (IMCNTs)

Figure 1 illustrates the modification of MWCNT, neat MWCNT shows the deformation D band at 1318 cm⁻¹, graphitic G band at 1575 cm⁻¹. The D band represents the defects present in CNTs owing to the minute amount of metal oxides and the G band corresponds to the hexagonal arrangement of carbon atoms. In addition, pristine MWCNT exhibits 2D band at 2635 cm⁻¹, it indicates that the electronic effects associated with graphitic carbon atoms. The increase in intensities and slight frequency shift of D and G band towards higher frequency were observed for IMCNT after the modification MWCNT with ionic liquid. The attributing factor for this is due to the ionic liquid can interact with CNT through π-π interactions [25, 26]; it clearly confirmed that CNT has been successfully modified. Moreover, the doping of ionic liquid can cause the increase in defects of MWCNT. Interestingly, increase in intensity and high frequency shift of 2D band of

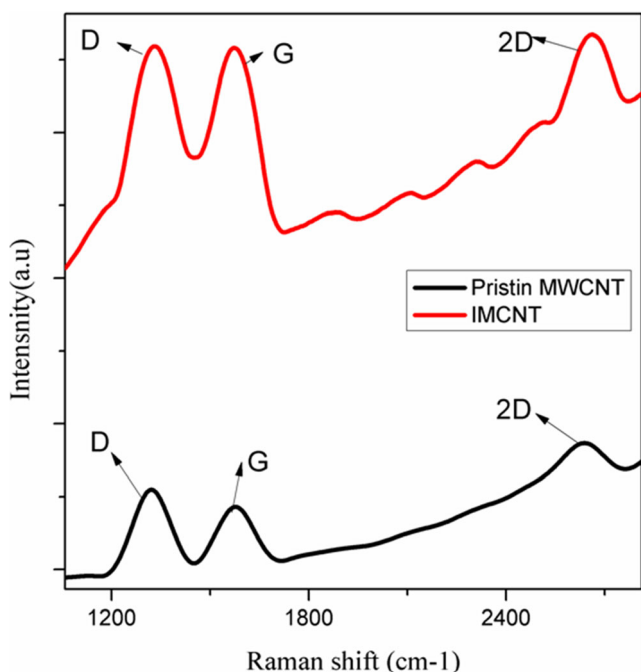


Fig. 1 Raman spectra of CNT and IMCNT

IMCNT also were noticed owing to charge transfer between ionic liquid and CNT.

Characterization of thermally reduced graphene oxide (TRG)

Raman spectrum unveils the transformation of graphite (GT) to TRG. The Raman spectrum of GT as shown in Fig. 2 indicates a small deformation D band (1343 cm^{-1}) and a strong graphitic G band (1573 cm^{-1}). D band reflects the deformations present in the GT and G band reveals the arrangement of carbons through cyclic ring structures. The position of the G band shifted in the order $\text{TRG} > \text{GO} > \text{GRT}$ owing to decrease in number of layers in solid state [27]. The 2D band of GT at 2715 cm^{-1} indicates overtone of the D band. After oxidation, comparing with raw GT, GO provides a significant enhancement in the intensity of D band while a decrease in the intensity of G band. It is confirmed that during functionalization of GT, the graphitic structure might be disturbed by the oxygen functionalities. Furthermore, the intensity of 2D band becomes broaden and decreased for GO and TRG indicating that presence of defects in graphitic materials [28]. Moreover, the intensity of D band and G band ratios (I_D/I_G) increases in the order from GT (0.12) to 0.96, 0.98 for GO and TRG and it clearly revealed that the transformation of TRG from GT has successfully been achieved.

XRD is an efficient tool to investigate the changes in graphitic materials and the results (Fig. 3) clearly confirm the changes from GT to TRG. The sharp peak at $2\theta \sim 27$ indicates the (002) plane (hexagonal arrangement of carbons) of GT. Oxidation of GT results in the shift of (002) peak to lower 2θ

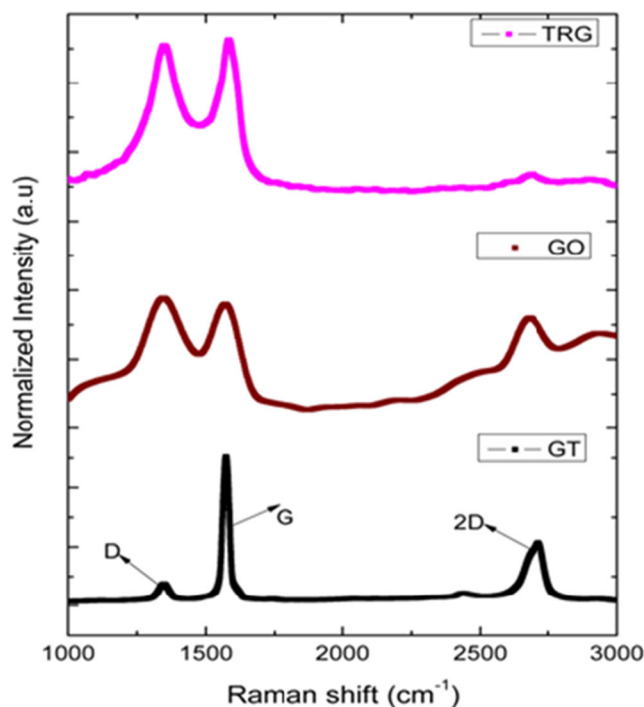


Fig. 2 Raman spectra of GT, GO and TRG

values which clearly indicates that the interlayer spacing between GT layers has been increased by the hydroxyl and acid groups of oxygen functionalities. After the reduction of GO, the peak (2θ value (10°)) disappeared and small hump at 2θ value (27°) retained as in the case of GT, providing an evidence that the TRG is an exfoliated state and also it clearly confirm that the as formed TRG contains a few layers of graphene.

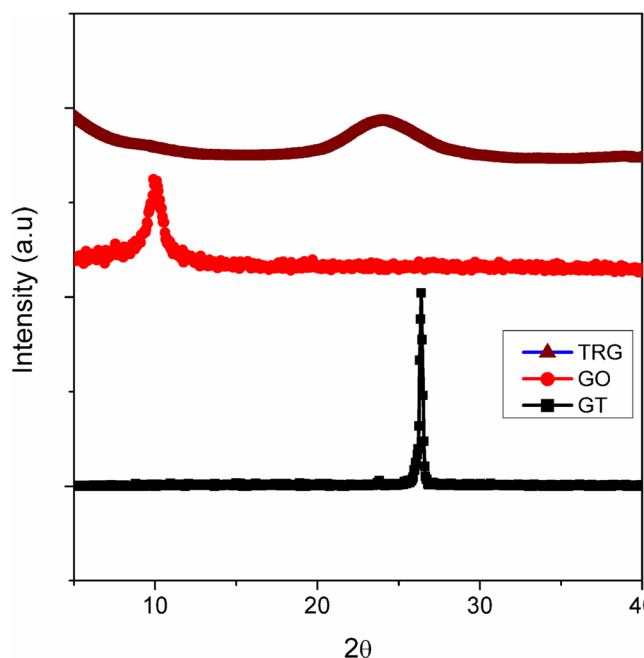


Fig. 3 XRD spectra of GT, GO and TRG

TEM micrographs of TRG are shown in Fig. 4, it can be clearly understood that the graphene layers have been successfully separated from GT. Thermal reduction process playing a crucial role in order to obtain fine attenuated TRG sheets. From the TEM images, it can be seen that the TRG contains mixed of few layers in the middle and edge portions. Supporting the TEM observations, XRD analysis of TRG shows a hump because of this combination of few layers of graphene. This is a clear evidence for the fact that graphene contains mixture of layers. Research reports had already been highlighted the wrinkled nature of graphene synthesized from graphite materials [23, 29].

Characterization of NR composites

The Fig. 5 illustrates the stress-strain behavior of the NR composites. From the Figure it is clear that the neat NR exhibits strain induced crystallization phenomena as expected. This is because of the stereo regularity of cis 1,4 polyisoprene units of NR. Consistent improvement in tensile strength and modulus were observed from the stress-strain curves of graphite (5 wt%), TRG (5 wt%) and hybrid (IMCNT+TRG) (5 wt%) filled NR composites as compared to neat NR. It is interesting to note that 5 wt% of hybrid (IMCNT+TRG) system showed high tensile strength, and modulus as compared to neat NR, graphite and TRG filled systems. Attributing factor for this behavior is due to the synergistic effect induced by the network formation between IMCNT and TRG throughout NR chains leading to high stress transfer from the filler to the NR chains. Similar kind of tensile properties were reported by Pots et al. [30] where they used NR latex stage compounding method. Moreover, the improvement in modulus is significantly contributed by the nano hybrid (IMCNT+

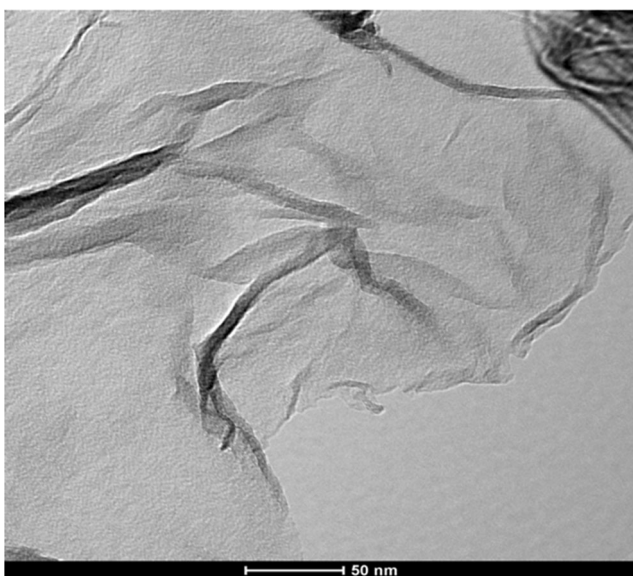


Fig. 4 TEM micrograph of thermally reduced graphene oxide (TRG)

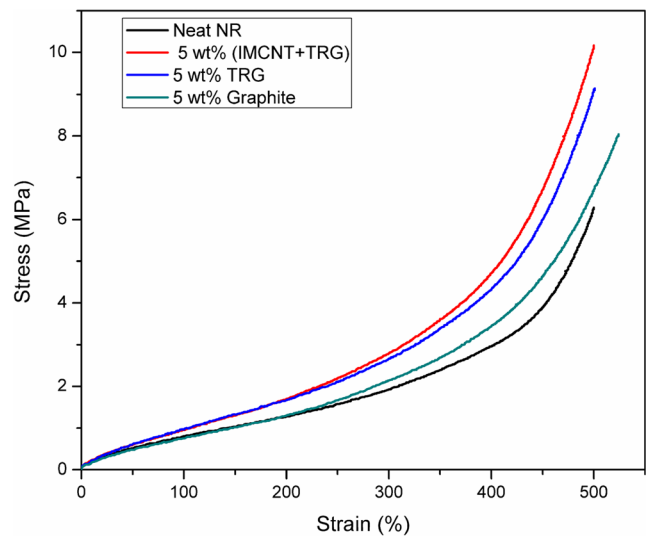


Fig. 5 Stress- strain curves of graphite, TRG and IMCNT+TRG filled NR composites

TRG) filler system and also the mechanical interlocking among the TRG, IMCNT and NR chains. Modulus data at different strains (100 and 300 %) are shown in Fig. 6. It is clear that from the figure that the modulus of graphite, TRG and IMCNT+TRG filled NR composites were higher than that of neat NR. Moreover, high modulus values are observed at 300 % strain owing to strain induced crystallization behavior of NR chains. Besides, the elongation at break of hybrid (IMCNT+TRG) system is lower than that of neat NR, graphite and TRG systems. This could be due to the surface of hybrid fillers sticking to the NR chains via non covalent interactions leading to the formation a rigid amorphous phase (RAF) which can resist the deformation of NR chains.

The dispersion pattern of nano fillers inside NR matrix was analyzed by X-ray diffraction. Figure 7 portrays the X-ray spectra of TRG and hybrid (TRG+IMCNT) filled NR composites. Interestingly, vulcanized neat NR exhibits peaks

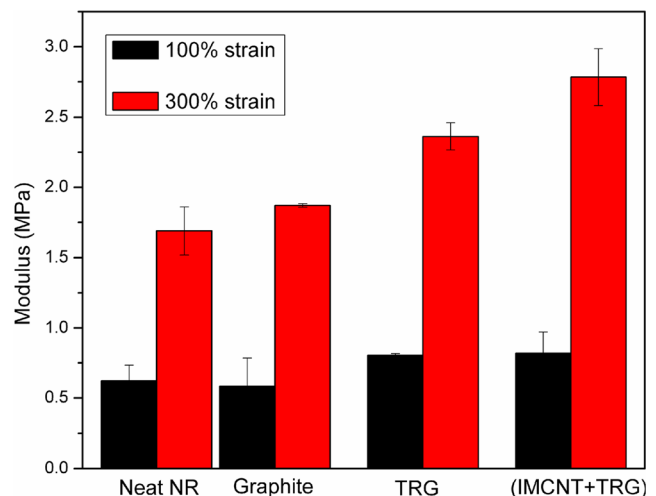
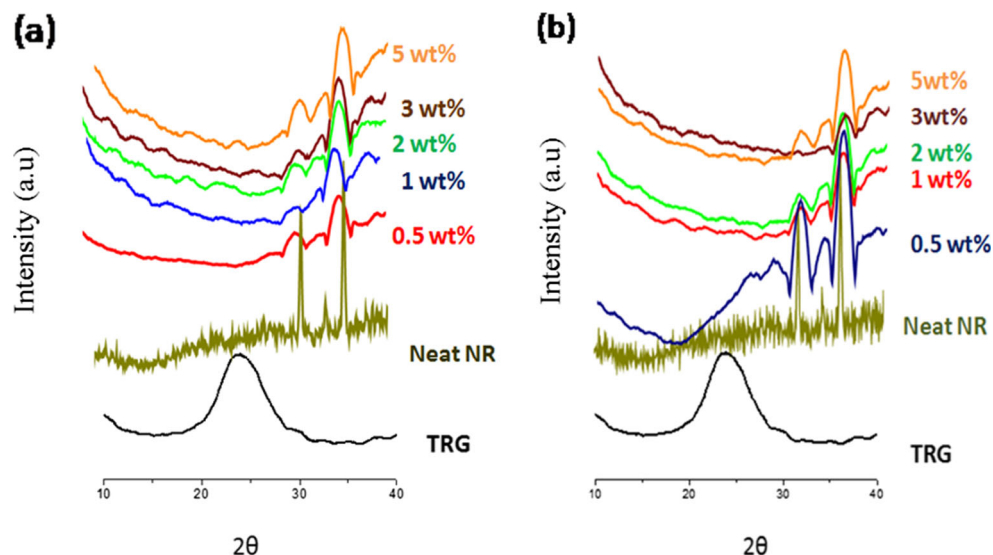


Fig. 6 Modulus of NR nano composites at various strains

Fig. 7 XRD spectra of NR composites **a** NR-TRG **b** NR-Hybrid (IMCNT+TRG)



((100) (022) (101)) at 2θ between 32 to 38° which are contributed by the ZnO curing agent [31, 32]. From the results, it can be noticed that with the addition of TRG nanofiller to the NR, the intensity of the characteristic peak of TRG at 27° decreases and or sometimes almost vanished, it implies that the nano filler exfoliated nicely inside a rubber matrix. In a similar manner, many reports have been revealed the state of dispersion of carbon fillers such as graphenes and CNTs inside the polymer matrix using XRD [33–35]. However, from XRD analysis, it is very difficult to distinguish the dispersion of the filler with respect to concentration.

TEM morphological micrographs are shown in Fig. 8; morphology of hybrid system (TRG+ IMCNT) at 5 wt% showed that IMCNT is acting as a bridge between TRG layers and thus the dispersion of TRG in NR phase is greatly improved by the IMCNTs. Consequently, we have

observed an improvement in dielectric properties as well as change in heat capacity of the hybrid system as compared to TRG and GT filled NR systems. In the case of TRG system, the TRG layers were not well dispersed as in the case of hybrid system. There was some sort of heterogeneous structure which emphasizes that it consists of both well dispersed and agglomerated regions inside the rubber phase. The attributing factor for establishing bridge structures and nice exfoliation of hybrid fillers inside the rubber phase may be due to the strong π - π interactions anchoring between CNT and TRG associated with ionic liquid. Moreover, TRG sheets acting as an auxiliary substance for CNT carrier and thus greatly restrict the inevitable aggregation of CNTs. In the TEM micrograph, red circles (Fig. 8a) represent the bridge formation between CNT and TRG, red arrow indicates the agglomerated region of TRG. While blue arrows (Fig. 8b) show

Fig. 8 TEM micrographs of selected NR composites **a** hybrid (IMCNT+TRG) at 5 wt% **b** TRG at 5 wt%

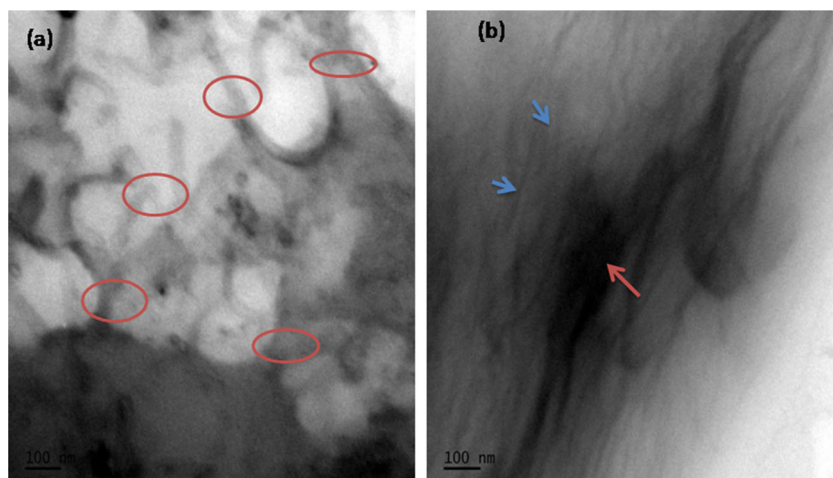
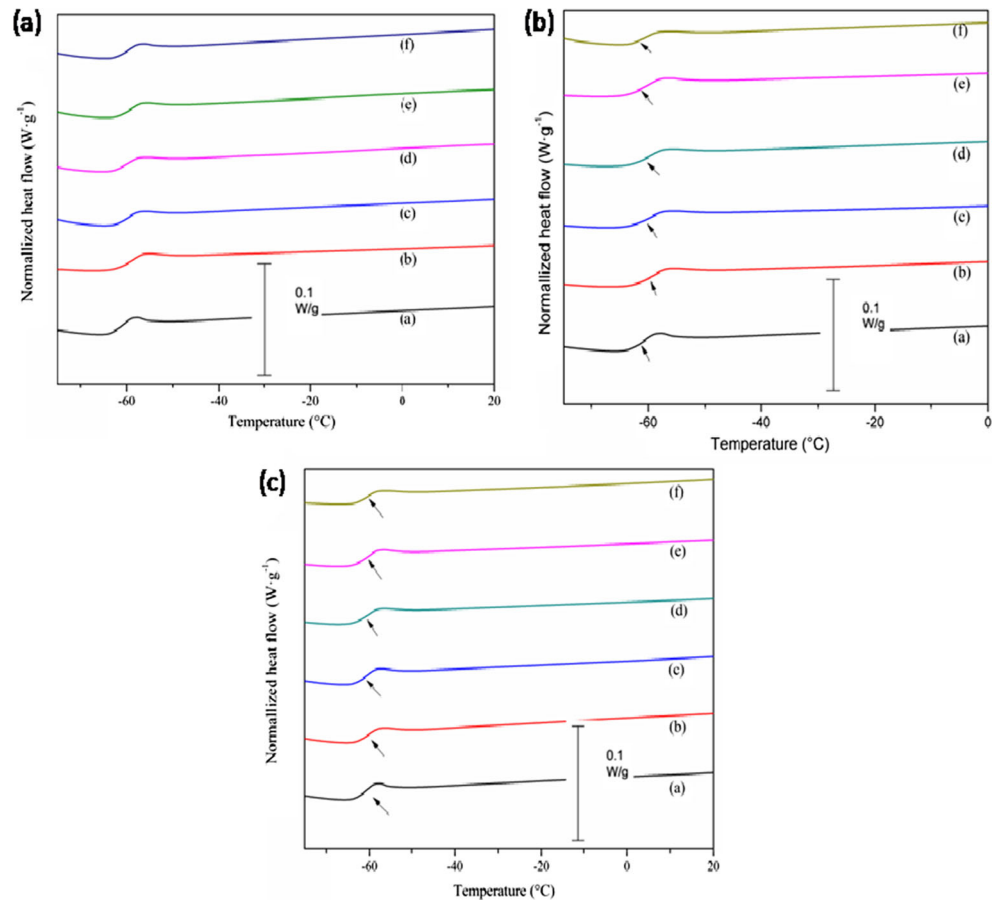


Fig. 9 DSC curves of NR composites **a** graphite-NR **b** TRG-NR **c** IMCNT+TRG-NR Inside images **(a)** Neat NR **(b)** 0.5 wt% **(c)** 1 wt% **(d)** 2 wt% **(e)** 3 wt% **(f)** 5 wt%



exfoliated region of TRG layers and it clearly supports that the TRG layers have been distributed in a heterogeneous manner in the NR matrix.

Thermal characteristics of GT, TRG and hybrid IMCNT+TRG filled NR composites were shown in Fig. 9. It can be noticed that there is not much significant changes in glass transition (T_g) of neat NR with the addition of fillers owing to high molecular weight of NR and also the filler concentration may not be sufficient to suppress the mobility of NR chains. However, there is a consistent decrease in change in heat capacity ΔC_p of the systems and these values are shown in Table 2. Generally, change in heat capacity associated with the segmental mobility of polymer chains. The attributing factor for decrease in change in heat capacity is that the filler may stick some portions of the NR polymer chains and leads to restricted segmental mobility of the NR chains. It clearly indicates the confinement of NR chains and the formation of rigid amorphous (RAF) phase at the surface of GT, TRG and IMCNT+TRG hybrid fillers. Among all systems, hybrid (IMCNT+TRG) system shows large decrease in change in heat capacity as compared to GT and TRG systems. Hybrid system comprising both TRG and IMCNT can exhibit a synergistic due to the nonpolar–non polar (π – π) interactions leading to the formation of a strong rigid amorphous phase (via

bridge network) resulting in good improvement in change in heat capacity. Research reports have revealed similar polymer

Table 2 Glass transition and heat capacity values of NR composites

Sample	T_g (onset)	T_g (endset)	T_g (mid)	ΔC_p (J/g°C)
NR	-63.4	-59.8	-61.7	0.52
TRG-(0.5 %)	-62.6	-57.3	-60.0	0.44
TRG-(1 %)	-62.9	-58.0	-60.5	0.44
TRG-(2 %)	-62.8	-58.0	-60.5	0.46
TRG-(3 %)	-63.0	-58.4	-60.8	0.47
TRG-(5 %)	-62.9	-58.7	-60.9	0.37
GT (0.5 %)	-62.0	-57.8	-60.1	0.42
GT (1 %)	-62.6	-58.9	-61.0	0.36
GT (2 %)	-63.3	-58.9	-61.6	0.40
GT (3 %)	-62.3	-58.8	-61.0	0.34
GT (5 %)	-62.8	-59.2	-61.5	0.36
TRG+ IMCNT(0.5 %)	-63.0	-59.5	-61.7	0.39
TRG+IMCNT (1 %)	-63.5	-59.9	-62.1	0.41
TRG+IMCNT (2 %)	-63.4	-59.5	-61.6	0.39
TRG+IMCNT (3 %)	-63.3	-59.5	-61.6	0.41
TRG+IMCNT (5 %)	-63.0	-59.7	-61.6	0.32

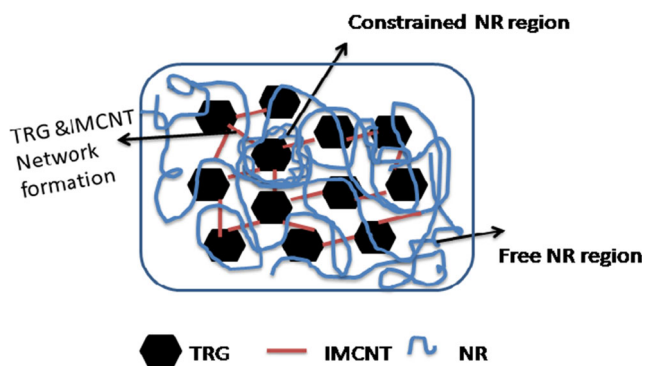


Fig. 10 Schematic representation of bridge formation of Hybrid (IMCNT+TRG) filled NR composite TRG+IMCNT(1:3) composites

chain confinement and the formation of rigid amorphous phase from ΔC_p measurements [36, 37]. Schematic representation of the bridge network formation, constrained and amorphous regions of NR-hybrid system is shown in Fig. 10.

Dielectric properties of GT, TRG and TRG+IMCNT filled NR composites are shown in Table 3. Dielectric measurements like dielectric constant and dielectric loss were carried out at microwave frequencies (2.5, 10 and 20 GHz). It is clear that with the addition of GT, TRG and hybrid TRG+IMCNT to NR, considerable improvement in dielectric constant can be obtained. Dielectric constant mainly related with the polarizability induced by the chemical composition when an oscillating electric field at a particular frequency is passed through it. In the case of TRG and IMCNT+TRG, dielectric constant values are higher than GT filled NR composites. This is because of

polarizability induced by the residual oxygen groups of TRG and also ionic liquid in MWCNT. However, the IMCNT+TRG hybrid system has shown high dielectric constant as compared to GT and TRG systems. This could be accomplished by synergistic effect of both IMCNT+TRG owing to polar residual oxygen groups of TRG and polar ionic liquid. Figure 11 shows the dielectric constant and loss tangent values with variation of frequency for hybrid NR (3 % w/w) TRG+IMCNT composites. This data has been generated using a linear fit analysis. The dielectric constant values decrease with increasing the frequencies from 2.5 to 20 GHz. At higher frequencies, the relaxation time of NR polymer chains is very long, and there is not sufficient time to relax the NR polymer coils when the microwave field passes through it as it varies at high frequencies, that is with short time periods. Moreover, higher loadings of fillers (5 wt%) results in a highly lossy or conducting behavior for the films at 10 and 20 GHz as the resonant behavior did not appear for the SPDR in these cases. In order to estimate the dielectric constant and loss at these microwave frequencies for such high lossy or conducting samples other measurement techniques will have to be used. Experiments are underway in this direction to evaluate the dielectric properties at higher loading. However, dielectric loss decreases reasonably in case of hybrid system as compared to TRG system. The GT system exhibits less loss compared to TRG and hybrid system. This is the result of reduced polarizability. Interestingly, with 5 wt% of hybrid system, it has shown a lower dielectric loss. It can be useful for flexible and hence wearable energy storage devices like capacitors.

Table 3 Dielectric properties of NR composites at microwave frequencies

S. no	Sample name	2.5 GHz		10 GHz		20 GHz	
		Dielectric constant	Loss tangent	Dielectric constant	Loss tangent	Dielectric constant	Loss tangent
1	Neat NR	2.7	0.012	2.5	0.0078	2.1	0.0068
2	(0.5 %) TRG	2.7	0.053	2.2	0.035	2.3	0.019
3	(1 %) TRG	3.2	0.030	2.4	0.035	2.5	0.020
4	(2 %) TRG	3.6	0.035	3.2	0.038	3.4	0.041
5	(3 %) TRG	3.7	0.046	3.4	0.040	3.5	0.051
6	(5 %) TRG	3.7	0.092	Sample is lossy or conducting		Sample is lossy or conducting	
7	(0.5 %) GT	2.9	0.087	2.68	0.0103	2.7	0.0105
8	(1 %) GT	3.0	0.010	2.60	0.0101	2.8	0.0214
9	(2 %) GT	3.2	0.011	2.91	0.0135	2.9	0.0150
10	(3 %) GT	3.4	0.012	2.90	0.0140	3	0.0206
11	(5 %) GT	3.0	0.015	3.70	0.0210	Sample is lossy or conducting	
12	(0.5 %) TRG+IMCNT(1:3)	2.9	0.019	2.6	0.016	2.6	0.016
13	(1 %) TRG+IMCNT(1:3)	3.5	0.027	3.2	0.025	3.1	0.028
14	(2 %) TRG+IMCNT(1:3)	3.7	0.031	3.0	0.020	3.3	0.045
15	(3 %) TRG+IMCNT(1:3)	4.7	0.043	3.2	0.044	3.4	0.046
16	(5 %) TRG+IMCNT(1:3)	5.6	0.026	Sample is lossy or conducting		Sample is lossy or conducting	

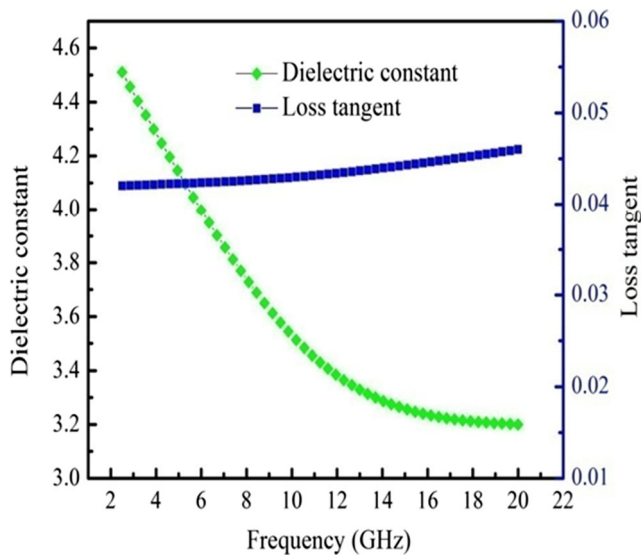


Fig. 11 Frequency dependence of dielectric properties of hybrid TRG+IMCNT(1:3) filled NR with (3 wt%)

To reveal the microwave absorption properties of hybrid system of IMCNT+TRG, the reflection loss (RL) values of IMCNT+TRG (3 % w/w) composites are calculated based on complex permittivity and permeability. According to transmission line theory [38], RL is given by

$$RL = 20\log \left| \frac{Z_{in} - Z_o}{Z_{in} + Z_o} \right| \tag{3}$$

Where,

$$Z_{in} = Z_o \sqrt{\frac{\mu_r}{\epsilon_r} \tanh \left[j \left(\frac{2\pi f d}{c} \right) \sqrt{\mu_r \epsilon_r} \right]} \tag{4}$$

Where, Z_o —is impedance of free space, Z_{in} —input impedance of the absorber, μ_r —complex permeability, ϵ_r —complex permittivity of medium, f —frequency of incident wave, d —thickness of absorber and c —velocity of electromagnetic wave in free space.

Figure 12 gives the frequency dependence of RL of IMCNT+TRG (3 wt%) composite with a variation of the thickness of the sample. The calculated reflection loss curve is above -2 dB for 0.5 mm thickness of the absorber. The microwave absorption intensity and peak position also strongly depend on the thickness of the absorber. The expected microwave absorption peak will be beyond the 20 GHz frequency. An approach possible to obtain the absorption peak in the required frequency range is to increase the thickness of the absorber. The RL value exceeding -2 and -10 dB is achieved at 20 GHz for 1.0 mm thickness of the absorber. Interestingly, the minimum reflection loss of -30 dB is obtained for the same absorber at the optimal thickness of 2.0 mm and -15 dB absorption is observed in the frequency range from 12 to 16 GHz.

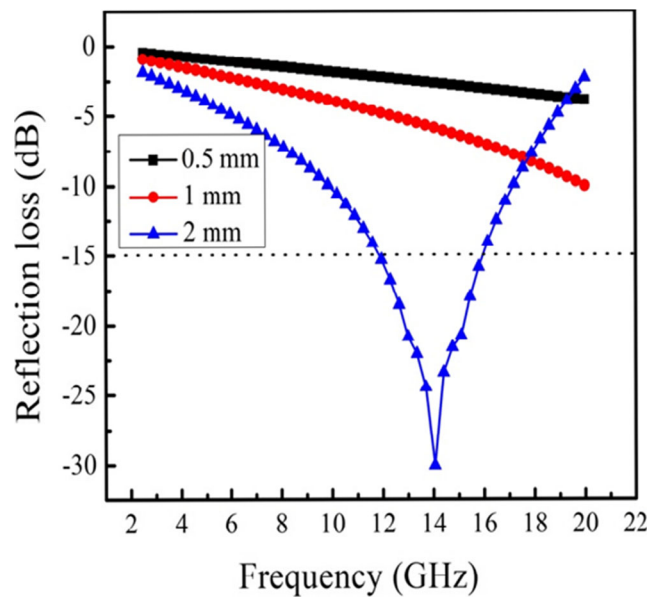


Fig. 12 Frequency dependence of reflection loss with various thickness of selected hybrid NR with (3 wt%) TRG+IMCNT(1:3) composites

Conclusions

Graphene has been prepared from Graphite via Hummer method and CNT was also successfully modified using ionic liquid. Fabrication of Graphite, TRG and hybrid (TRG+IMCNT) filled NR films was done using environment friendly melt mixing method using Haake. Mechanical testing of NR composites (5 wt%) clearly revealed the synergistic effect of hybrid (TRG+IMCNT) system owing to the formation of networking inside the NR matrix. Dielectric properties like dielectric constant and loss tangent values are reported at microwave frequencies. Hybrid system (TRG+IMCNTs) exhibits high dielectric constant values and lower loss tangent values as compared to TRG system owing to the polarity induced by residual oxygen functionalities of TRG and ionic liquid from IMCNT. In certain cases, with the filler at 5 wt% concentration, the films showed high loss or conducting behavior at higher frequencies (10 and 20 GHz). Different techniques had to be used for measuring the dielectric constant and loss tangent of the prepared membranes where they showed a high loss or conducting behavior. Moreover, the change in heat capacity values clearly unveiled that the hybrid system (IMCNT+TRG) interacted more through nonpolar–non polar interactions, thereby homogeneous distribution of the filler was achieved through TRG & CNT bridge network formation. It could be clearly observed from morphological micrographs of the systems. Overall, the hybrid system (IMCNT+TRG) has strong efficacy to perform better dielectric and thermal properties as compared to graphite and TRG systems. The lossy compositions have been identified as useful materials for microwave absorption applications while the non lossy compositions are useful for energy storage devices like capacitors.

Acknowledgments We would like to express our sincere thanks to UGC, New Delhi, DST Nanomission and Universiti Teknologi MARA, Shah Alam, Malaysia for the financial support.

References

- Brosseau C, Boulic F, Queffelec P et al (1997) Dielectric and microstructure properties of polymer carbon black composites. *J Appl Phys* 81:882–890
- Li ZH (2008) Effects of carbon blacks with various structures on vulcanization and reinforcement of filled ethylene-propylene-diene rubber. *Express Polym Lett* 2:695–704
- Wang C, Guo Z-X, Fu S et al (2004) Polymers containing fullerene or carbon nanotube structures. *Prog Polym Sci* 29:1079–1141
- Dennler G, Scharber MC, Brabec CJ (2009) Polymer-fullerene bulk-heterojunction solar cells. *Adv Mater* 21:1323–1338
- Szczepanik M, Stabik J, Dybowska A (2009) Influence of graphite on electrical properties of polymer composites. *Arch Mater Sci Eng* 37:37–44
- Compton OC, Kim S, Pierre C, Torkelson JM, Nguyen ST (2010) Crumpled graphene nanosheets as highly effective barrier property enhancers. *Adv Mater* 22:4759–4763
- Moazzami Gudarzi M (2012) Enhancement of dispersion and bonding of graphene-polymer through wet transfer of functionalized graphene oxide. *Express Polym Lett* 6:1017–1031
- Vega JF, Martínez-Salazar J, Trujillo M et al (2009) Rheology, processing, tensile properties, and crystallization of polyethylene/carbon nanotube nanocomposites. *Macromolecules* 42:4719–4727
- Bokobza L (2012) Multiwall carbon nanotube-filled natural rubber: electrical and mechanical properties. *Express Polym Lett* 6:213–223
- Ismail H, Pasbakhsh P, Fauzi MNA, Abu Bakar A (2008) Morphological, thermal and tensile properties of halloysite nanotubes filled ethylene propylene diene monomer (EPDM) nanocomposites. *Polym Test* 27:841–850
- Tang W, Santare MH, Advani SG (2003) Melt processing and mechanical property characterization of multi-walled carbon nanotube/high density polyethylene (MWNT/HDPE) composite films. *Carbon* 41:2779–2785
- Montazeri A, Javadpour J, Khavandi A et al (2010) Mechanical properties of multi-walled carbon nanotube/epoxy composites. *Mater Des* 31:4202–4208
- Phang IY, Shen L, Chow SY, Zhang W-D (2004) Morphology and mechanical properties of multiwalled carbon nanotubes reinforced nylon-6 composites. *Macromolecules* 37:7214–7222
- Müller MT, Krause B, Kretschmar B, Pötschke P (2011) Influence of feeding conditions in twin-screw extrusion of PP/MWCNT composites on electrical and mechanical properties. *Compos Sci Technol* 71:1535–1542
- Deng Y, Li Y, Dai J et al (2011) Functionalization of graphene oxide towards thermo-sensitive nanocomposites via moderate in situ SET-LRP. *J Polym Sci A Polym Chem* 49:4747–4755
- Rafiee MA, Rafiee J, Srivastava I et al (2010) Fracture and fatigue in graphene nanocomposites. *Small* 6:179–183
- Graphene A, Qi X, Pu K et al (2010) Amphiphilic graphene composites. *Angew Chem Int Ed* 49:9426–9429
- Wu T, Pan Y, Liu E, Li L (2012) Carbon nanotube/polypropylene composite particles for microwave welding. *J Appl Polym Sci* 126: 283–289
- Theilmann P, Chu KM, Bandaru PR et al (2012) Optimisation of microwave absorption of carbon nanotube composites through use of carboxyl-epoxide functional group linkages. *Electron Lett* 48: 638
- Bhattacharya P (2013) Microwave absorption behaviour of MWCNT based nanocomposites in X-band region. *Express Polym Lett* 7:212–223
- Al-Hartomy OA, Al-Ghamdi A, Al-Salamy F et al (2012) Dielectric and microwave properties of graphene nanoplatelets/carbon black filled natural rubber composites. *Int J Mater Chem* 2:116–122
- Al-Hartomy OA (2012) Dielectric and microwave properties of natural rubber based nanocomposites containing graphene. *Mater Sci Appl* 03:453–459
- Subrahmanyam KS, Vivekchand SRC, Govindaraj A, Rao CNR (2008) A study of graphenes prepared by different methods: characterization, properties and solubilization. *J Mater Chem* 18:1517
- Krupa J, Gregory AP, Rochard OC, Clarke RN, Riddle B, Baker-Jarvis J (2001) Uncertainty of complex permittivity measurements by split-post dielectric resonator technique. *J Eur Ceram Soc* 21: 2673–2676
- Fukushima T, Kosaka A, Ishimura Y, Yamamoto T, Takigawa T, Ishii N, Aida T (2003) Molecular ordering of organic molten salts triggered by single-walled carbon nanotubes. *Science* 300(5628): 2072–2074
- Wang J, Chu H, Li Y (2008) Why single-walled carbon nanotubes can be dispersed in imidazolium-based ionic liquids. *ACS Nano* 2(12):2540–2546
- Rao CNR, Biswas K, Subrahmanyam KS, Govindaraj A (2009) Graphene, the new nanocarbon. *J Mater Chem* 19:2457–2469
- Chieu TC, Dresselhaus MS (1982) Raman studies of benzene-derived graphite fibers. *Phys Rev B* 26:5867–5877
- Chen M, Park C, Choi J, Oh W (2011) Synthesis and characterization of metal (Pt, Pd and Fe)-graphene composites. *J Korean Ceram Soc* 48:147–151
- Potts JR, Shankar O, Du L, Ruoff RS (2012) Processing–morphology–property relationships and composite theory analysis of reduced graphene oxide/natural rubber nanocomposites. *Macromolecules* 45:6045–6055
- Lv Y, Yu L, Huang H et al (2012) Application of the soluble salt-assisted route to scalable synthesis of ZnO nanopowder with repeated photocatalytic activity. *Nanotechnology* 23:065402
- Panigrahy B, Aslam M, Bahadur D (2012) Effect of Fe doping concentration on optical and magnetic properties of ZnO nanorods. *Nanotechnology* 23:115601
- Kishor S, Castro M, Saiter A et al (2013) Development of poly (isobutylene-co-isoprene)/reduced graphene oxide nanocomposites for barrier, dielectric and sensing applications. *Mater Lett* 96:109–112
- Potts JR, Shankar O, Murali S et al (2013) Latex and two-roll mill processing of thermally-exfoliated graphite oxide/natural rubber nanocomposites. *Compos Sci Technol* 74:166–172
- Ponnamma D, Sadasivuni KK, Strankowski M et al (2013) Synergistic effect of multi walled carbon nanotubes and reduced graphene oxides in natural rubber for sensing application. *Soft Matter* 9:10343–10353
- Jose JP, Thomas S (2014) Alumina-clay nanoscale hybrid filler assembling in cross-linked polyethylene based nanocomposites: mechanics and thermal properties. *Phys Chem Chem Phys* 16: 14730–14740
- Thomas SP, Thomas S, Bandyopadhyay S (2009) Polystyrene calcium phosphate nanocomposites : preparation, morphology, and mechanical behavior polystyrene. *J Phys Chem C* 113(1):97–104
- Guo J, Wang X, Liao X, Zhanga W, Shi B (2012) Skin collagen fiber-biotemplated synthesis of size-tunable silver nanoparticle-embedded hierarchical intertextures with lightweight and highly efficient microwave absorption properties. *J Phys Chem C* 116: 8188–8195